Aerospace Science and Technology, 1999, no. 3, 177–189

μ Tools for flight control robustness assessment

C. Döll[a,b,*], G. Ferreres[a], J.-F. Magni[a]

[a] ONERA-DCT/DCSD, Systems Control and Flight Dynamics Department, BP 4025, 31055 Toulouse cedex 04, France
[b] SUPAERO Ecole Nationale Supérieure de l'Aéronautique et de l'Espace, BP 4032, 31055 Toulouse cedex 04, France

(Received 9 October 1998, revised 21 December 1998, accepted 5 February 1999)

Döll C., Ferreres G., Magni J.-F., *Aerospace Science and Technology*, 1999, no. 3, 177–189

Abstract

The aim of this paper is to emphasize the usefulness of the μ framework for the analysis of the robustness properties of flight control systems. Model uncertainties may correspond, either to parametric uncertainties (e.g. in the aerodynamic model or in the value of the trim point) or to neglected high frequency dynamics (e.g. in the actuators or sensors). We especially show that several classical problems (computation of a phase or delay margin, non-linear analysis of a PIO effect, computation of a frequency domain overshoot) can be extended to an uncertain aircraft model. A flexible model of the aircraft can, moreover, be taken into account. © Elsevier, Paris

robustness / μ framework / flexible structures / phase and delay margins / non-linear analysis

Résumé

Évaluation de la robustesse de lois de pilotage avec les outils de μ-analyse. Le but de cet article est de mettre en valeur la μ-analyse pour caractériser la robustesse et les performances des systèmes de pilotage. Les incertitudes de modèle correspondent, soit aux incertitudes paramétriques (induites par le modèle aérodynamique ou le point d'équilibre), soit aux dynamiques négligées aux hautes fréquences (dûes aux actionneurs ou capteurs). Plus précisement, on montre que plusieurs problèmes classiques (tels que le calcul d'une marge de phase ou de retard, l'analyse non-linéaire du phénomène de pompage piloté, le calcul du dépassement dans le domaine fréquentiel) peuvent être étendus à un modèle d'avion incertain. En outre, un modèle flexible d'avion peut aussi être pris en compte. © Elsevier, Paris

robustesse / μ-analyse / structures flexibles / marges de phase et de retard / analyse non-linéaire

Glossary

LFT: Linear Fractional Transformation
LMI: Linear Matrix Inequality
LTI: Linear Time Invariant
MIMO: Multi Input Multi Output
SIDF: Sinusoidal Input Describing Function
SISO: Single Input Single Output
s.s.v.: structured singular value

* Correspondence and reprints

1. Introduction

Performance analysis in the presence of uncertainties is a major issue in aeronautics. Indeed, aircraft models depend on several parameters, which are either measured, or only known to lie between some bounds. The key problem is then to check the stability and performance properties of the controlled aircraft in the face of all these possible parameter variations. This validation must be ideally done in all the flight domain, and more realistically in a relevant part of this domain.

As illustrated in this paper, μ-analysis (see [27, 30, 31] and the references therein) appears to be a suitable framework for that problem. The application of this technique is done in two steps. The first one is to derive a standard form for the parametrically uncertain aircraft, while the second one is to apply classical (and less classical) computational tools to this standard form. The first step appears to be a difficult task (see [29]), since numerous uncertain parameters may enter into the aircraft model in a rather complex way. For example, a standard form of an aircraft may indeed depend on:

- Potentially uncertain parameters, such as the aircraft mass, the position of the center of gravity or the coefficients of the aerodynamic model.
- Steady-state values of state variables which describe a trim condition: these may, for example, correspond to the aircraft speed or to its angle of attack.
- Parameters which are used to schedule the feedback controller as a function of the operating point.
- Uncertainties in the parameters of a pilot model (when trying, for example to, detect a PIO effect).
- Non-linearities such as rate limiters or saturations in the actuators models.

A first obvious solution is to check the stability and performance properties on each point of a gridding, in the space of all possible parameter variations. Such an analysis may however be computationally infeasible, since the number of points in the gridding increases exponentially with the number of parameters.

μ–analysis appears as an alternative efficient method for a "one shot" analysis of the robust stability and performance properties, over the continuum of models which is described by the standard form. On the one hand, this technique enables us to guarantee that the studied property is actually satisfied over the whole continuum of models [1]. This technique may moreover provide worst case values of the parameters, i.e. values corresponding to the worst degradation of the performance property which is to be studied.

[1] On the contrary, when gridding the space of parameters, it can not be claimed that a worst case closed loop behaviour has not been missed, which would correspond to a value of the parameters between two points of the gridding.

Since μ–analysis is now a well known tool, we refer to the literature for the most classical ways to use it (see e.g. [1, 15]), and we prefer to emphasize the usefulness of the μ tools for specific problems, which are related to aeronautical applications:

- *Introduction of the flexible part of the aircraft in the robustness analysis problem*: this issue appears especially crucial when considering large dimension transport aircraft, since the frequencies of the bending modes become very close to the control bandwidth, and it is no longer possible to consider these flexible modes as neglected dynamics [9]. It appears especially necessary to adapt the standard computational μ tools to this new problem.

- *Computation of a worst case phase or delay margin in the presence of model uncertainties*: it is indeed important to validate the control law with respect to uncertainties in the time delays, since these delays occur at various locations of the flight control system (flight computer and sensors). Uncertainties in the physical parameters of the aircraft are moreover to be taken into account in such an analysis. Assuming that all parameter variations are bounded inside a given hypercube, the μ tools enable us to find the worst case value of the phase or delay margin together with the worst case value of the parameters inside the hypercube [14].

- *Linear (category I) analysis of a PIO effect in the presence of model uncertainties*: a criterion for ensuring the absence of a linear pilot-in-the-loop oscillation (PIO) phenomenon [6] consists in minimizing the frequency domain overshoot of a selected transfer. We illustrate in this paper that μ analysis enables to compute the worst case frequency domain overshoot of an uncertain transfer.

- *Non-linear (category II) analysis of a PIO effect in the presence of model uncertainties*: non-linearities such as rate limiters are now inserted into the linear model of the closed loop aircraft (possibly augmented with a pilot model), see [5, 6] and references therein. The μ tool can be used as a basis for techniques, which either ensure the absence of limit-cycles, or detect the presence of limit-cycles in the face of model uncertainties [12]. In a classical way, non-linearities are replaced by their equivalent gains, and the issue is for example to find the largest size parameter hypercube, inside which it can be guaranteed that no limit-cycle arises.

The paper is organized as follows. Section 2 introduces the μ framework, contains notations and briefly introduces the tools (μ, skewed μ and one-sided skewed μ measures). Section 3 presents the 4 specific problems which appear to be of particular interest in this paper. The last section is devoted to the computational issues.

2. Introduction to the μ framework

2.1. A generic example

As a preliminary, we only recall the definition of upper and lower LFTs. Let H and Δ denote, either complex matrices, or transfer matrices. The lower LFT $F_l(H, \Delta)$ (resp. the upper LFT $F_u(H, \Delta)$) represents the uncertain transfer between u and y, which is obtained when closing the Δ loop in *figure 1a* (resp. in *figure 1b*).

We can now introduce the μ framework with the following example. Let $y = F_l(H(s), \Delta)u$ the LFT standard form, which corresponds to the LTI uncertain open loop model of the aircraft. u represents the control inputs (e.g. the elevator deflection in the case of a longitudinal model) and y the feedback outputs (e.g. the vertical acceleration and pitch rate). As explained in [29], the parametric uncertainties in the structured model perturbation Δ is a real diagonal matrix of the form:

$$\Delta = \mathrm{diag}(\delta_1 I_{q_1}, \ldots, \delta_N I_{q_N}). \qquad (1)$$

The real scalar δ_i, which is said to be repeated if $q_i > 1$, corresponds to the normalized uncertainty in the ith physical parameter of the aircraft, and $\delta_i = 0$ corresponds to the nominal value of this parameter. As an example, if δ_1 corresponds to the aircraft mass, $\delta_1 \in [-1, 1]$ may for example mean that the mass varies between $\pm$ 20 % around its nominal value (depending on the freely chosen constant which is used to normalize the range of possible variations of the mass).

In the context of aeronautical problems, the family of models obtained by closing in *figure 1a* the Δ-loop with admissible matrices Δ (see equation (1)) is thus the continuum of linearized models, which corresponds to the set of possible values for the physical parameters of the aircraft model.

Connect then the open loop LFT model of the aircraft with the flight control law $K(s)$, as shown in *figure 2a*. This uncertain closed loop system can then be put under the generic form of *figure 2b*, which is called a standard interconnection structure $M(s) - \Delta$. $M(s)$ is simply the transfer which is seen by the real model perturbation Δ in *figure 2a*, i.e. the transfer between w and z. We emphasize the equivalence of both figures, i.e. in the case of our example, *figure 2b* is just an other way to represent *figure 2a*.

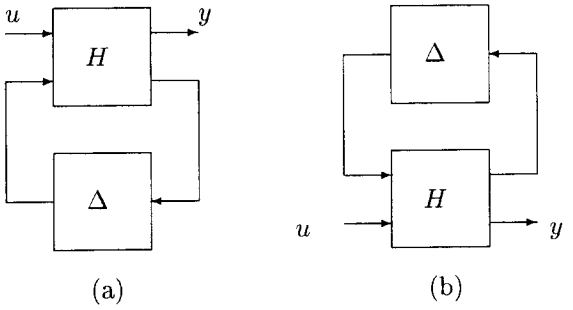

Figure 1. Lower and upper LFTs.

Let D the unit hypercube in the space of the δ_i's:

$$D = \{\delta \mid \delta_i \in [-1, 1]\ \forall i \in [1, N]\}. \qquad (2)$$

With some abuse of notation, $\Delta \in D$ should be understood in the following as $\delta \in D$, where Δ is defined in equation (1).

The nominal closed loop system (i.e. the one corresponding to $\Delta = 0$ in *figure 2a* or *2b*) is assumed to be asymptotically stable. Our aim is then to compute the robustness margin $k_{\max} > 0$, defined as the maximal value of k, such that the uncertain closed loop of *figure 2a* or *2b* remains asymptotically stable for all $\Delta \in kD$. In other words, the uncertain closed loop is guaranteed to be stable for all δ_i varying independently inside the interval $[-k_{\max}, k_{\max}]$.

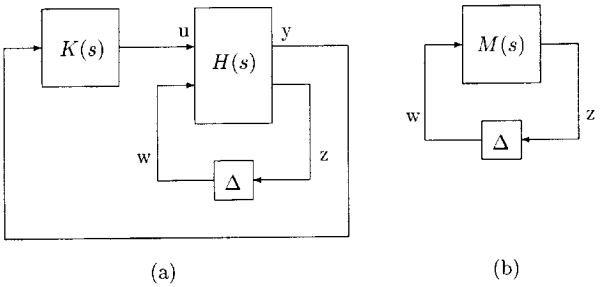

Figure 2. (a) Uncertain closed loop system, (b) standard interconnection structure for μ-analysis.

Assume that the parameters δ_i belong to the hypercube kD, where k increases from 0. By assumption, all poles of the uncertain closed loop are inside the left half plane for $k = 0$. On the other hand, for a sufficiently large value of k, at least some poles of the uncertain closed loop are now inside the right half plane (except in the special case of an infinite robustness margin $k_{\max}$).

Using a continuity argument, when k increases from 0, it can be claimed that the uncertain closed loop becomes marginally stable (i.e. all poles inside the left half plane, except one or more poles on the imaginary axis) before being unstable. As a consequence, the principle of μ analysis is to find the minimal size model perturbation Δ, which moves one closed loop pole onto the imaginary axis.

More precisely, let $\dfrac{1}{\mu(M(j\omega))}$ be the magnitude of the minimal size model perturbation Δ, which shifts one closed loop pole onto the imaginary axis at $j\omega$. Let us redefine the robustness margin $k_{\max}$ in this sense as the magnitude of the model perturbation Δ which shifts

one closed loop pole somewhere onto the imaginary axis. Then we obtain:

$$k_{\max} = \min_{\omega\in[0,\infty]} \frac{1}{\mu(M(j\omega))} = \frac{1}{\max\limits_{\omega\in[0,\infty]} \mu(M(j\omega))}. \quad (3)$$

μ-analysis is thus a frequency domain technique, which computes the s.s.v. $\mu(M(j\omega))$ as a function of frequency ω. The robustness margin $k_{\max}$ is then deduced.

Following the classical generalized Nyquist criterion, it suffices now to remark that the closed loop of *figure 2b* has a pole at the point s_0 of the complex plane if and only if $\det[I - M(s_0)\Delta] = 0$. As a consequence, $\frac{1}{\mu(M(j\omega))}$ is defined as the magnitude of the minimal size model perturbation Δ, which renders the matrix $\det[I - M(j\omega)\Delta] = 0$ singular.

2.2. Notations

• Our notation is the same as in [27, 30, 31]. As a preliminary, we define a block of neglected dynamics $\Delta^C(s)$ as an uncertain transfer matrix, which is only known to satisfy the H_∞ inequality:

$$\|\Delta^C(s)\|_\infty < 1 \iff \overline{\sigma}\left[\Delta^C(j\omega)\right] < 1 \ \forall\omega \in [0,\ \infty]. \quad (4)$$

At a given frequency ω, $\Delta^C(s)$becomes thus a full complex block $\Delta^C(j\omega)$, i.e. a complex matrix without specific structure which is only known to satisfy $\overline{\sigma}(\Delta^C(j\omega)) < 1$.

• Generally speaking, it is possible to transform a closed loop system subject to parametric uncertainties and blocks of neglected dynamics into the standard interconnection structure $M(s) - \Delta(s)$ of *figure 2b*. As illustrated in the example of the previous subsection, $M(s)$ contains the nominal closed loop system as well as the way the various model uncertainties enter the closed loop, while $\Delta(s)$ gathers all these model uncertainties. At a given frequency ω, the structured model perturbation $\Delta(s)$ becomes a complex matrix which has the following specific structure:

$$\Delta = \mathrm{diag}\,(\Delta_1, \ldots, \Delta_r) \quad (5)$$

in which Δ_i may be, either a diagonal matrix of the form $\Delta_i = \delta_i I_{q_i}$ with $\delta_i \in \mathbb{R}$ (a real repeated scalar block accounting for the parameter uncertainties), or a matrix in $\mathbb{C}^{n_i\times n_i}$ without specific structure (a full complex block accounting for neglected dynamics). The model perturbations Δ which have the above structure will be called in the following *admissible model perturbations*.

In μ-analysis, the size of this structured model perturbation Δ is classically defined as $\overline{\sigma}(\Delta)$. Consider the simplified case of a model perturbation $\Delta = \mathrm{diag}(\delta, \Delta^C)$, where δ is a real scalar while Δ^C is a full complex block: as a key property of the spectral norm $\overline{\sigma}$, the inequality $\overline{\sigma}(\Delta) \le 1$ is equivalent to $\delta \in [-1, 1]$ and $\overline{\sigma}(\Delta^C) \le 1$.

Note also that the structured model perturbation Δ may be real (if it only contains parametric uncertainties), complex (if it only contains full complex blocks) and otherwise mixed (if it simultaneously contains real and complex uncertainties). In the same way, the associated s.s.v. is said to be real, complex or mixed.

• Let there be a complex matrix M, which typically corresponds to the value of the transfer matrix $M(s)$ at $s = j\omega$. *The μ "measure"* of M is then defined as:

$$\mu(M) = 1/\overline{\sigma}(\Delta) \quad (6)$$

where Δ is the minimal size admissible model perturbation which satisfies $\det(I - M\Delta) = 0$. This definition is illustrated in *figure 3a*: Δ is chosen as $\Delta = \mathrm{diag}(\delta_1, \delta_2)$, where the δ_i's are real, and the line in *figure 3* corresponds to the equality $\det(I - M\Delta) = 0$. In the space of the δ_i's, the μ measure consequently corresponds to the inverse of the size of the largest square around the zero point, inside which $\det(I - M\Delta) \neq 0$.

• Let $\Delta = \mathrm{diag}(\Delta_1, \Delta_2)$ be split into two structured model perturbations Δ_1 and Δ_2. The maximal size of Δ_1 is fixed, typically $\overline{\sigma}(\Delta_1) < 1$. *The skewed μ "measure"* is then defined as:

$$\nu(M) = 1/\overline{\sigma}(\Delta_2) \quad (7)$$

where $\Delta = \mathrm{diag}\,(\Delta_1, \Delta_2)$ is an admissible model perturbation which satisfies $\overline{\sigma}(\Delta_1) < 1$ and $\det(I - M\Delta) = 0$ and the norm of Δ_2 is minimal (possibly larger than 1). This definition is illustrated in *figure 3b*. δ_1 is maintained inside $[-1,\ 1]$, while the size of δ_2 is to be maximized as long as the system remains stable.

• Assume that Δ_2 reduces to a single real repeated block $\Delta_2 = \delta_2 I_{q_2}$, which is to be expanded on just one side. Some uncertainties have indeed to be physically positive, such as uncertain delays. *The one-sided skewed μ "measure"* is then defined as:

$$\nu^{os}(M) = 1/\delta_2 \quad (8)$$

where the admissible model perturbation $\Delta = \mathrm{diag}(\Delta_1, \delta_2 I_{q_2})$ satisfies $\overline{\sigma}(\Delta_1) < 1$, $\det(I - M\Delta) = 0$ and the norm of $\delta_2 > 0$ is minimal (possibly larger than 1). This definition is illustrated in *figure 3c*. Here again, δ_1 is maintained inside $[-1,\ 1]$, while the size of δ_2 is to be maximized in the positive direction as long as the system remains stable.

3. Some criteria revisited

3.1. Robustness analysis of flexible structures

When applying μ-analysis to the standard interconnection structure $M(s) - \Delta$ of *figure 2b*, the s.s.v.

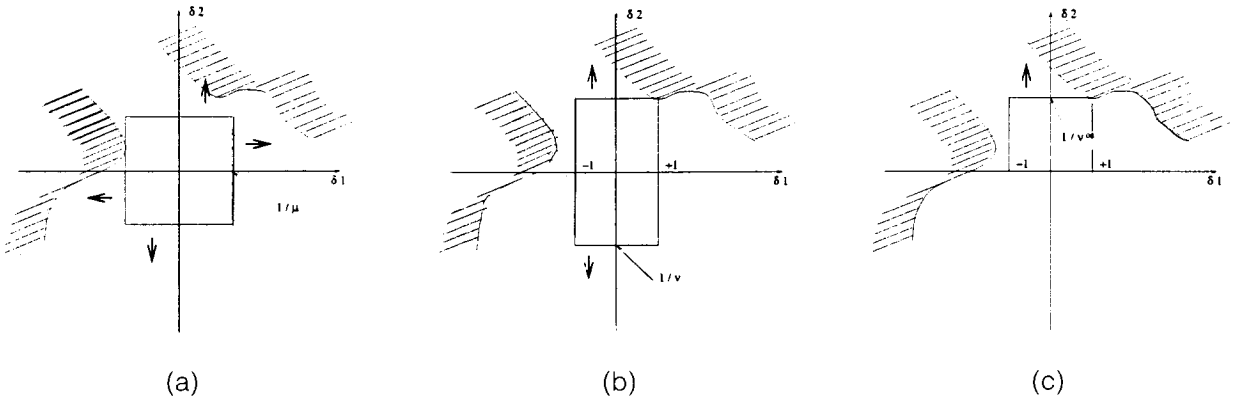

Figure 3. (a) Illustration of the definition of the μ measure, (b) illustration of the definition of the skewed μ measure ν, (c) illustration of the definition of the one-sided skewed μ measure ν^{os}.

$\mu(M(j\omega))$ should be computed on the continuum of frequencies $\omega \in [0, \infty]$, and the robustness margin is then obtained using equation (3). The most usual solution is nevertheless to compute $\mu(M(j\omega))$ at each point of a frequency gridding, and to make a regularity assumption concerning the variation of μ between the neighboring frequency points.

This solution usually provides good results, except in some special cases: when considering especially systems with lightly damped modes, it is possible to obtain narrow and high peaks on the μ plot, so that only a prohibitively fine frequency gridding could find them. An attractive solution in this case is to directly compute the maximal s.s.v. over the frequency range, or – more interestingly – over small intervals corresponding to the peaks of the μ plot.

A first idea is to consider an augmented μ problem, in which the frequency ω is treated as an additional parametric uncertainty: a skewed μ problem [11] or a one–sided skewed μ problem [16] is then obtained. This approach, despite its simplicity, appears however computationally cumbersome in the case of high order transfer matrices $M(s)$. As a consequence, in subsections 4.2.1. and 4.3.2., we will rather focus on alternative approaches, which are computationally more efficient and which have delivered good results in practical examples [4, 9, 17].

3.2. Worst case phase and delay margin computation

The computation of a delay margin is a practically important problem, since more and more flight control system realizations are digital. As a consequence, time-delays are to be accounted for at the controller outputs as well as at the sensor outputs. It is moreover necessary to take into account classical model uncertainties (i.e. real parametric uncertainties and neglected dynamics) in the computation of the delay margin.

Consider again the open loop aircraft model $F_l[H(s), \Delta_2]$, where the real model perturbation Δ_2 gathers all parametric uncertainties (see *figure 4*). Connect this model with the flight controller $K(s)$ and add at the plant input a phase block $e^{-j\phi}$, which will be used to represent an uncertain time-delay $e^{-\tau s}$ at $s = j\omega$. $\phi = 0$ (or $\tau = 0$) and $\Delta_2 = 0$ correspond to the nominal closed loop, which is assumed to be asymptotically stable.

The idea is to compute at each frequency ω the worst case value $\phi^*(\omega)$ of the classical SISO phase margin (i.e. the minimal value of the phase margin, which is obtained when the parametric uncertainties in Δ_2 belong to the unit hypercube). The corresponding delay margin is then deduced as $\tau(\omega) = \dfrac{\phi^*(\omega)}{\omega}$. Let then $\tau^* = \min_\omega \tau^*(\omega)$ be the worst case delay margin; it can be claimed that the closed loop is asymptotically stable for all values of the time-delay $\tau \in [0, \tau^*]$ and for all parametric uncertainties in Δ_2 inside the unit hypercube.

Note that we consider for the sake of simplicity the case of a single time delay, but that our method can be extended to the general case of a closed loop system, which is simultaneously subject to classical model uncertainties (parametric uncertainties and neglected dynamics) and to several uncertain time-delays [14].

The closed loop of *figure 4* is first equivalently rewritten as the interconnection structure of *figure 5a*. We

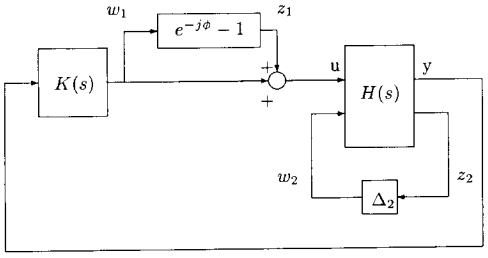

Figure 4. An uncertain closed loop with time delay.

then precisely define at each frequency ω the notion of worst case phase margin as the maximal value $\phi^*(\omega)$ of $\phi(\omega)$, such that:

$$\det\left(I - P_1(j\omega)\begin{bmatrix} e^{-j\phi} - 1 & 0 \\ 0 & \Delta_2 \end{bmatrix}\right) \neq 0 \qquad (9)$$

for all $\phi \in [0,\ \phi(\omega)]$ and for all admissible model perturbations Δ_2 satisfying $\overline{\sigma}(\Delta_2) < 1$.

The issue is now to compute at each frequency ω the worst case phase margin $\phi^*(\omega)$ defined above. The idea is to replace $e^{-j\phi}$ by a real scalar δ using:

$$e^{-j\phi} = \frac{1 - j\delta}{1 + j\delta}. \qquad (10)$$

The unit circle, which corresponds to $\phi \in [0,\ 2\pi]$, is completely described when $\delta \in [-\infty, +\infty]$. Note especially that $\delta \in [0,\ +\infty]$ is equivalent to the lower half circle of *figure 6*.

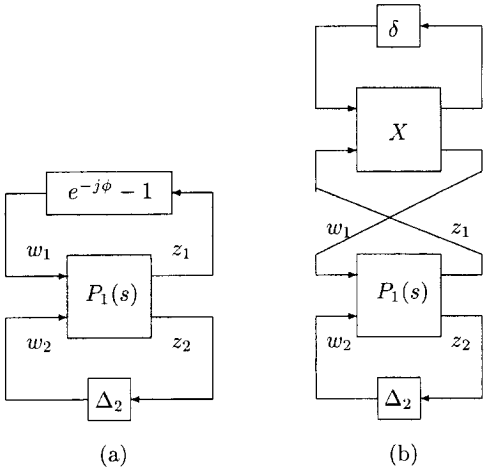

Figure 5. New interconnection structure for the uncertain closed loop with time delay.

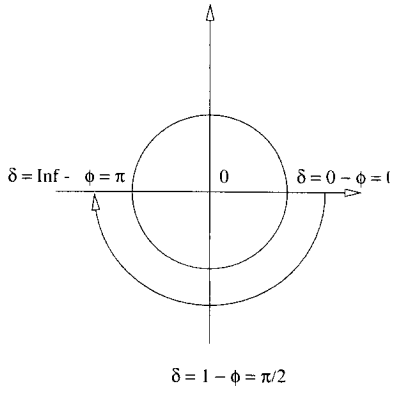

Figure 6. Representation of $e^{-j\phi} = \dfrac{1 - j\delta}{1 + j\delta}$ in the complex plane.

We would like to realize $e^{-j\phi} - 1 = \dfrac{-2j\delta}{1 + j\delta}$ as an LFT transfer $F_u(X, \delta)$, where X is a two dimensional matrix:

$$X = \begin{bmatrix} a & b \\ c & d \end{bmatrix} \qquad (11)$$

so that:

$$F_u(X, \delta) = \frac{d + \delta(cb - ad)}{1 - a\delta}. \qquad (12)$$

When comparing with $e^{-j\phi} - 1 = \dfrac{-2j\delta}{1 + j\delta}$, the coefficients of X are identified as:

$$X = \begin{bmatrix} -j & 1 \\ -2j & 0 \end{bmatrix}. \qquad (13)$$

When replacing $e^{-j\phi} - 1$ by its LFT realization $F_u(X, \delta)$, the interconnection structure of *figure 5a* is equivalently transformed into the one of *figure 5b*. This new interconnection structure can then be rewritten as the classical interconnection structure of *figure 2b*, in which $\Delta = \text{diag}(\delta, \Delta_2)$ only contains the initial structured model perturbation Δ_2 and an additional parametric uncertainty δ. Because of the equivalence of the transformation of *figure 4* into *figure 2b*, equation (9) is equivalent, under some technical assumptions, to:

$$\det\left(I - M(j\omega)\begin{bmatrix} \delta & 0 \\ 0 & \Delta_2 \end{bmatrix}\right) \neq 0. \qquad (14)$$

The problem of computing the worst case phase margin has been consequently recast into a standard μ problem involving the model perturbation $\Delta = \text{diag}(\delta, \Delta_2)$.

A one–sided skewed μ problem has been more precisely obtained. Our aim is indeed to compute the maximal value $k_{\max}$ of k, such that equation (14) is satisfied for all $\delta \in [0,\ k]$ and for all admissible model perturbations Δ_2 satisfying $\overline{\sigma}(\Delta_2) < 1$. $\phi^*(\omega)$ is then deduced from $k_{\max}$ as:

$$\begin{aligned} \phi^*(\omega) &= \arctan\frac{2k_{\max}}{1 - k_{\max}^2} && \text{for } k_{\max} \in [0,\ 1[\\ \phi^*(\omega) &= \frac{\pi}{2} && \text{for } k_{\max} = 1 \\ \phi^*(\omega) &= \pi + \arctan\frac{2k_{\max}}{1 - k_{\max}^2} && \text{for } k_{\max} \in]1,\ \infty]. \end{aligned} \qquad (15)$$

Remark: see [14] for the practical implementation of the method, which is more complex. Note especially that if $\phi^*(\omega) > \pi$, the upper half circle is considered in the same way as the lower half circle, simply by multiplying equation (10) by $e^{j\pi} = -1$.

3.3. Frequency domain overshoot analysis

3.3.1. A technical result

We briefly present a technical result, which will play a key role in the rest of section 3. Let H a given complex matrix and Δ_2 an admissible model perturbation. We

would like to solve the following robust performance problem, namely to check whether the norm of the LFT transfer $y = F_l(H, \Delta_2)\, u$ of *figure 7a* remains less than 1, i.e. whether $\overline{\sigma}[F_l(H, \Delta_2)] < 1$ for all admissible model perturbations Δ_2 satisfying $\overline{\sigma}(\Delta_2) < 1$.

Consider the augmented μ problem of *figure 7b*, in which Δ_1 represents an additional full complex block. The *Main Loop Theorem* [27] claims that, under some technical conditions, $\overline{\sigma}[F_l(H, \Delta_2)] < 1$ for all admissible model perturbations Δ_2 satisfying $\overline{\sigma}(\Delta_2) < 1$ if and only if $\mu_\Delta(H) < 1$, where $\Delta = \mathrm{diag}(\Delta_1, \Delta_2)$.

Assume now that we would like to compute the maximal value $k_{\max}$ of k, such that the norm of the LFT transfer $y = F_l(H, \Delta_2)\, u$ of *figure 7a* remains less than 1 for all admissible model perturbations Δ_2 satisfying $\overline{\sigma}(\Delta_2) < k$.

Introducing here again an additional full complex block Δ_1 in *figure 7b*, and using a *skewed version* of the classical *Main Loop Theorem* (see [10]), it can be proved that $k_{\max}$ can be obtained as:

$$\frac{1}{k_{\max}} = \nu(H) \tag{16}$$

accordingly to equation (7), i.e. the size k of the structured model perturbation Δ_2 is to be maximized ($\overline{\sigma}(\Delta_2) < k$), whilst the size of the fictitious complex block Δ_1 remains less than 1 ($\overline{\sigma}(\Delta_1) < 1$).

3.3.2. *Frequency domain overshoot analysis*

Consider again the LFT transfer $y = F_l[H(s), \Delta_2]\, u$ of *figure 7a*. This may correspond, either to an open loop transfer such as the parametrically uncertain aircraft model, or to a closed loop transfer. Our objective is then to analyze the worst case overshoot of the normalized frequency response between the vector input u and the vector output y, when the admissible model perturbation satisfies $\overline{\sigma}(\Delta_2) < 1$, i.e. all normalized parametric uncertainties $\delta_i \in [-1, 1]$ if $\Delta_2 = \mathrm{diag}(\delta_i I_{q_i})$.

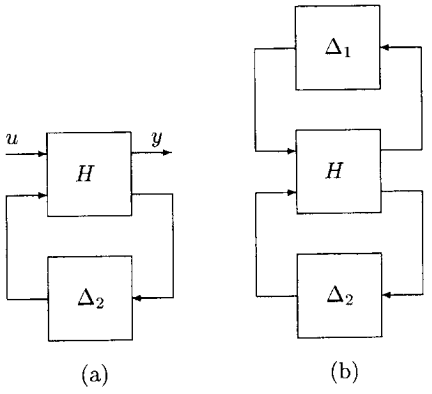

Figure 7. An augmented skewed μ problem.

A first solution is to use the technical result of subsection 3.3.1. A more sophisticated solution takes into account the fact that this overshoot depends on the static gain $F_l[H(0), \Delta_2]$. The issue is now to check whether the worst case overshoot is less than a given positive real number L, i.e. whether the following relation is satisfied for all admissible model perturbations Δ_2 satisfying $\overline{\sigma}(\Delta_2) < 1$:

$$\overline{\sigma}\left(\frac{1}{L}\,\frac{F_l[H(j\omega), \Delta]}{F_l[H(0), \Delta]}\right) < 1. \tag{17}$$

A realization of the transfer $\dfrac{1}{L}\,\dfrac{F_l[H(s), \Delta]}{F_l[H(0), \Delta]}$ is proposed in *figure 8a*, as the transfer between $\tilde{u}$ and $\tilde{y}$. Let $\tilde{\Delta} = \mathrm{diag}(\Delta_2, \Delta_2)$. The transfer of *figure 8a* can then be rewritten as the LFT transfer $\tilde{y} = F_l\left[\tilde{P}(s), \tilde{\Delta}\right]\tilde{u}$ of *figure 8b*, i.e. Δ_2 is now repeated twice in the new structured model perturbation $\tilde{\Delta}$.

It suffices now to apply the technical result of subsection 3.3.1. to the LFT transfer $F_l\left[\tilde{P}(j\omega), \tilde{\Delta}\right]$, i.e. to consider a new augmented model perturbation $\Delta = \mathrm{diag}(\Delta_1, \tilde{\Delta})$, where Δ_1 is a fictitious full complex block.

3.4. Limit-cycles analysis

3.4.1. *A technical result*

We first introduce a technical result, which will be used afterwards. Consider the interconnection structure of *figure 7b*, and partition H compatibly with the Δ_i's as:

$$H = \begin{bmatrix} H_{11} & H_{12} \\ H_{21} & H_{22} \end{bmatrix}. \tag{18}$$

As a consequence:

$$F_l(H, \Delta_2) = H_{11} + H_{12}\Delta_2\,(I - H_{22}\Delta_2)^{-1}\,H_{21} \tag{19}$$

$$F_u(H, \Delta_1) = H_{22} + H_{21}\Delta_1\,(I - H_{11}\Delta_1)^{-1}\,H_{12}. \tag{20}$$

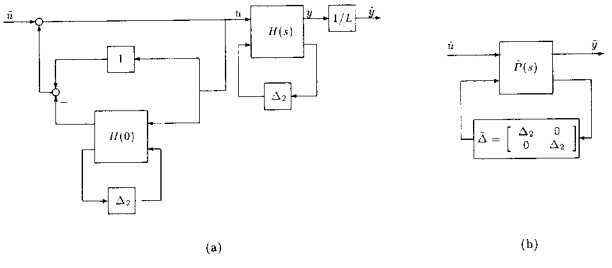

Figure 8. LFT representation for overshoot analysis (a) normalized (b) final.

Using classical properties of the determinant, and especially the fact that:

$$\det\left(\begin{bmatrix} A & B \\ C & D \end{bmatrix}\right) = \det(A)\det\left(D - CA^{-1}B\right) \quad (21)$$

where A, B, C, D are complex matrices of suitable dimensions, it can be proved that:

$$\det\left(I - H\begin{bmatrix} \Delta_1 & 0 \\ 0 & \Delta_2 \end{bmatrix}\right)$$
$$= \det(I - H_{22}\Delta_2)\det(I - F_l[H, \Delta_2]\Delta_1)$$
$$= \det(I - H_{11}\Delta_1)\det(I - F_u[H, \Delta_1]\Delta_2).$$

As a consequence, under the assumption that $\det(I - H_{11}\Delta_1) \neq 0$ and $\det(I - H_{22}\Delta_2) \neq 0$, the following key property is obtained:

$$\det\left(I - H\begin{bmatrix} \Delta_1 & 0 \\ 0 & \Delta_2 \end{bmatrix}\right) \neq 0$$
$$\Longleftrightarrow \det(I - F_l[H, \Delta_2]\Delta_1) \neq 0$$
$$\Longleftrightarrow \det(I - F_u[H, \Delta_1]\Delta_2) \neq 0. \quad (22)$$

Refering to the definition of the s.s.v. in section 2.2., equation (22) can be treated by the computation of the μ-measure. Noting that $\mu(M) = \overline{\sigma}(M)$ if the model perturbation is a full complex block, equation (22) appears to be the basis of the classical *Main Loop Theorem* of section 3.3.1.

3.4.2. *Non-linear analysis*

Consider now the closed loop system of *figure 9a*. Here again, the LFT transfer $F_l[H(s), \Delta_2]$ represents the parametrically uncertain aircraft model, while $K(s)$ is the flight control system. Φ represents a non-linearity such as a rate limiter or a saturation on the controller output. *Note that for the sake of clarity, we thus consider in the following the case of a single MIMO non-linearity* Φ. *The method which we present can be nevertheless extended to the general case of several MIMO non-linearities occurring at various locations of the closed loop [12].*

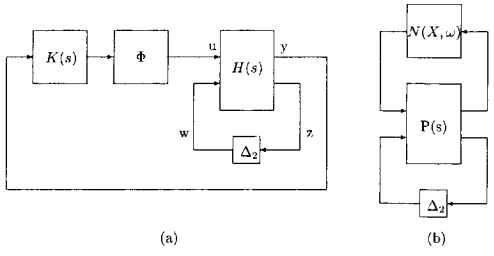

Figure 9. Interconnection structure to detect limit-cycles in the presence of LTI parametric uncertainties.

We first introduce the classical Sinusoidal Input Describing Function (SIDF) $N(X, \omega)$ of a SISO non-linearity Φ (the definition can be readily extended to the case of a MIMO non-linearity). A sinusoidal input $u(t) = X\sin(\omega t)$ is applied to Φ. The output of the non-linearity, which is supposed to have odd symmetry, can be written as:

$$y(t) = P\sin(\omega t) + Q\cos(\omega t) + \epsilon(t) \quad (23)$$

where $\epsilon(t)$ contains the super-harmonic part of the signal $y(t)$. The SIDF is then classically introduced as the gain:

$$N(X, \omega) = \frac{P + jQ}{X}. \quad (24)$$

In the context of the first harmonic approximation, the closed loop signal $\epsilon(t)$ is typically assumed to be filtered by the low-pass transfers $F_l[H(s), \Delta_2]$ and $K(s)$.

As a *first problem*, we would like to detect a limit-cycle in the presence of parametric uncertainties in Δ_2. To this aim, the MIMO non-linearity Φ is replaced by its corresponding gain matrix $N(X, \omega)$ in the closed loop system of *figure 9a*, and the new closed loop system of *figure 9b* is obtained (in which $P(s)$ represents an interconnection of the transfer matrices $H(s)$ and $K(s)$). Under the assumption that the first harmonic approximation above is valid, a very classical necessary condition for the existence of a limit-cycle with magnitude X and frequency ω is:

$$\det(I - N(X, \omega)\, F_l[P(j\omega), \Delta_2]) = 0. \quad (25)$$

Using the method of subsection 3.4.1., it can be noted that then equation (25) is satisfied if and only if:

$$\det(I - F_u[P(j\omega), N(X, \omega)]\,\Delta_2) = 0, \quad (26)$$

X and ω are fixed. The issue is then to find the minimal size of the model perturbation Δ_2, which satisfies the above equation. This size is obviously given by

$$\frac{1}{\mu(F_u[P(j\omega), N(X, \omega)])}.$$

As a *second problem*, we would like to compute the maximal amount of parametric uncertainties in Δ_2, for which it can be guaranteed that no limit-cycle occurs. The non-linearity Φ is now replaced by $N(X, \omega) + \Delta_1$ in the closed loop system of *figure 9a*, and *figure 10a* is obtained. Roughly speaking, Δ_1 may be considered as a block of neglected dynamics, which is used to take into account the super-harmonic part $\epsilon(t)$ of the signal $y(t)$. Δ_1 is only known by the relation:

$$\overline{\sigma}(\Delta_1) < \alpha(X, \omega) \quad (27)$$

where $\alpha(X, \omega)$ is a known function of the magnitude X and frequency ω of the limit-cycle. For the sake of simplicity, we assume $\alpha(X, \omega) = 1$ in the following.

Figure 10a is then reshaped into *figure 10b*. A sufficient condition for the absence of limit-cycles in the

closed loop is then given by the following weak gain condition, which is to be satisfied for all admissible model perturbations Δ_2:

$$\overline{\sigma}\,(F_l\,[Q(X,\omega),\,\Delta_2]) < 1. \qquad (28)$$

Remember $F_l[Q(X,\omega),\,\Delta_2]$ corresponds to the LFT transfer between w and z in *figure 10b* with $\Delta_1 = 0$. For given values of X and ω, the problem consequently reduces to the problem of computing the maximal amount of parametric uncertainties in Δ_2, for which the sufficient condition (28) for the absence of limit-cycles remains satisfied. Using the technical result of subsection 3.3.1., an augmented skewed μ problem is obtained, which involves the augmented model perturbation $\Delta = \mathrm{diag}(\Delta_1, \Delta_2)$.

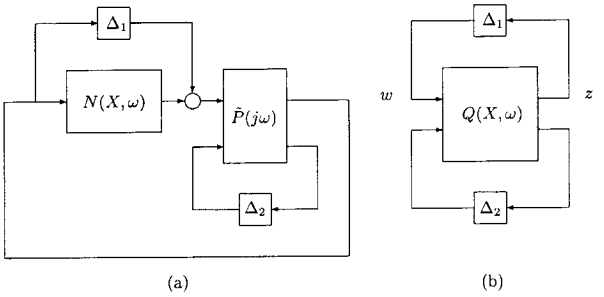

Figure 10. Interconnection structure to guarantee that no limit-cycles occur in the presence of LTI parametric uncertainties.

4. Computation of μ bounds

4.1. Introduction

Many methods exist for computing μ. Before briefly presenting a few methods in the following subsections, note that these techniques can be classified using various criteria:

- The algorithm may be exponential-time or polynomial-time, i.e. its computational effort may be an exponential or polynomial function of the number of uncertainties. Note that the computation of the structured singular value μ is a NP-hard problem, so that any algorithm which computes the exact value of μ is exponential-time. As a consequence, for large dimension problems, lower and upper bounds are computed for μ, instead of the exact value, using polynomial-time algorithms.
- The algorithm provides, either the exact value of μ, or a μ lower bound, or a μ upper bound.
- Some algorithms are just applicable to special classes of model uncertainties. A great deal of work has been especially devoted to the computation of the real (or the bounds of the real) s.s.v., i.e. only parametric uncertainties can be dealt with. Conversely, some methods only deal with complex uncertainties (typically neglected dynamics at various locations of the closed loop).
- The algorithm can compute a μ bound, either at a given frequency ω, or directly over the frequency range (using thus a frequency sweeping technique, as in subsections 4.2.1. and 4.3.2.; see also section 3.1. for its motivation).

4.2. μ lower bound computation

4.2.1. Frequency sweeping techniques

As already mentioned in section 3.1. one possibility to treat the μ–computation without frequency gridding is to consider the frequency as an additional uncertainty. The problem is that the frequency will then be a real uncertainty δ repeated as many times as the number of states of the considered system. Obviously, this approach will be computationally cumbersome in the case of high order systems.

A new algorithm (called later *algorithm 1*) which computes a lower bound of the peaks of the μ curve is introduced in [4, 21]. This algorithm is efficient for mixed or purely real uncertainties. From the fact that frequency gridding is not used, the proposed polynomial-time algorithm is very fast and the risk to miss high, narrow peaks due to flexible structures is minimized. This is quite useful in a design cycle in which it is necessary to detect worst cases; see [20] in this issue and [24].

The idea beyond this technique consists in shifting the eigenvalues towards the imaginary axis with a minimum norm perturbation. An adaptation of the *pole migration technique* of [23] is used. The proposed algorithm is divided into two steps. After the first step the limit of stability (i.e. the imaginary axis) is reached with a model perturbation of minimum Frobenius norm. The second step consists in minimizing the 'sigma-max norm' of the perturbation obtained after the first step while remaining at the limit of stability.

4.2.2. Pointwise computation

See [30] for the so-called polynomial-time *Standard Power Algorithm SPA*. It computes a mixed μ lower bound at a given frequency ω via a fixed-point algorithm. The application of the SPA is restricted by the use of frequency gridding and convergence problems provoked by limit-cycles (especially with real and repeated complex scalars). In [26, 28] convergence improvements are proposed at the cost of increasing computational time.

Two different combinations of [30] with the approach of the previous section exist:

- Initialization of the SPA with the results of the Frobenius norm optimization algorithm, see also [22].

- The method proposed in [9]: First, the so-called regularized μ problem is solved (i.e. adding some complex scalars to improve the convergence characteristics of the SPA). A mixed model perturbation matrix Δ'' is obtained which renders the closed loop system marginally stable. Its complex parts are omitted, hence the resulting model perturbation matrix Δ' does not render the system unstable anymore. An LP algorithm, based on the approach of the previous section, is used to adjust Δ' so that the system becomes again unstable. The smallest destabilizing model perturbation matrix Δ is obtained. This algorithm will be called *algorithm 2*.

In [3] an exponential-time algorithm is proposed which is restricted to real uncertainties and based on frequency gridding.

4.3. μ upper bound computation

4.3.1. Pointwise computation

See [27, 31] for the polynomial-time computation of a complex or mixed μ upper bound with frequency gridding.

Two sets of scalings are considered having the same structure as Δ, see (5):

- $\mathcal{D}$: $\boldsymbol{D}_i = \boldsymbol{D}_i^* > 0$ and $\boldsymbol{D}_i \in \mathbb{C}^{n_i \times n_i}$ for real and complex repeated blocks. $\boldsymbol{D}_i = d_i I_{n_i}$ and $d_i > 0$ for full complex blocks. $\boldsymbol{D} \in \mathcal{D}$ is consequently a positive definite matrix;
- $\mathcal{G}$: $\boldsymbol{G}_i = \boldsymbol{G}_i^*$ and $\boldsymbol{G}_i \in \mathbb{C}^{n_i \times n_i}$ for real repeated blocks. $\boldsymbol{G}_i = 0$ for other blocks. $\boldsymbol{G} \in \mathcal{G}$ is an hermitian block diagonal matrix,

or respectively:

- $\widehat{\mathcal{D}}$: $\det(\widehat{D}_i) \neq 0$ and $\widehat{D}_i \in \mathbb{C}^{n_i \times n_i}$ for real and complex repeated blocks. $\widehat{D} = d_i I_{n_i}$ and $d_i \neq 0$, $d_i \in \mathbb{C}$ for full complex blocks. $\widehat{D} \in \widehat{\mathcal{D}}$ is not anymore positive definite;
- $\widehat{\mathcal{G}}$: $\widehat{G} = \mathrm{diag}(g_i)$ and $g_j \in \mathbb{R}$ for real repeated blocks. $\widehat{G} = 0$ for other blocks. $\widehat{G} \in \widehat{\mathcal{G}}$ is a real diagonal matrix.

We shall use the following well known result (see [31]).

Lemma 4.1. *The Laplace variable s being fixed, let $\boldsymbol{D} \in \mathcal{D}$, $\boldsymbol{G} \in \mathcal{G}$ and β be such that*

$$M^H(s)\boldsymbol{D}M(s) + j\left[\boldsymbol{G}M(s) - M^H(s)\boldsymbol{G}\right] \leq \beta^2 \boldsymbol{D} \quad (29)$$

then

$$\mu(M(s)) \leq \beta. \quad (30)$$

The problem of finding the best upper bound β of $\mu(M(s))$ is equivalent to the problem of minimizing β under the LMI condition of equation (29). It is known as a (quasi-convex) generalized eigenvalue problem: For fixed $\boldsymbol{D}$ and $\boldsymbol{G}$ the problem recasts to an eigenvalue problem, and if β is fixed a priori, it is possible to find $\boldsymbol{D}$ and $\boldsymbol{G}$ satisfying (29) by solving an LMI as the problem becomes linear (and hence convex) in $\boldsymbol{D}$ and $\boldsymbol{G}$. The scalings $\boldsymbol{D}$ and $\boldsymbol{G}$ and the best β are determined at all points of a frequency gridding.

In [31] an alternative formulation of the μ upper bound is derived:

Lemma 4.2. *The Laplace variable s being fixed, let $\widehat{D} \in \widehat{\mathcal{D}}$, $\widehat{G} \in \widehat{\mathcal{G}}$ and β be such that*

$$\overline{\sigma}\left[F^{-1/4}\left(\frac{\widehat{D}M(s)\widehat{D}^{-1}}{\beta} - j\widehat{G}\right)F^{-1/4}\right] \leq 1 \quad (31)$$

with $F = I + \widehat{G}^2$, then

$$\mu(M(s)) \leq \beta.$$

This second equivalent formulation involves the minimization of a singular value $\overline{\sigma}$. As a consequence, the mixed μ upper bound can be computed, either using efficient methods for solving LMIs [2], or using a specific algorithm which takes into account the particular structure of the optimization problem [31].

A completely different exponential–time algorithm applying frequency gridding for a real μ upper bound is proposed in [19]. At least in the pure real case, it delivers a better upper bound than the algorithm of [27].

4.3.2. Frequency sweeping techniques

See [11, 16, 18] for preliminary methods based on the consideration of an augmented μ problem which consists in treating the frequency ω as an additional parametric uncertainty. This will at least be repeated as many times as there are system states so that the computation becomes difficult, even impossible for high order systems.

Hence, the following two new algorithms are cited. They are based on the same idea.

We take advantage of the knowledge of the lower bounds of peak values of μ. Let $\mu_{\max}$ be the highest lower bound available. In order to validate this result say with 10 % accuracy, it suffices to consider a test value $\mu_T = 1.1\,\mu_{\max}$ and to check that μ is lower than this value for all frequencies.

Thus the problem consists in finding intervals of frequencies for which a given pair of scalings $\boldsymbol{D}_0$ and $\boldsymbol{G}_0$ (see section 4.3.1.) enables us to conclude that μ is less than μ_T. For a graphical determination of these intervals see [25] and the example treated in section 5.

A *first analytical description of these intervals* is derived in [8] and is based on the μ upper bound formulation as the singular value minimization of lemma 4.2. The corresponding algorithm will be called *algorithm 3*.

A *second analytical derivation of these intervals* based on the μ upper bound formulation as the minimization of a generalized eigenvalue problem of lemma 4.1. is given in [25]. In the following we will speak of *algorithm 4*.

The main idea is that checking equation (30) with $\beta = \mu_T$ on a frequency interval $\omega \in [\omega^- \ \omega^+]$ around ω_0 reduces to finding the eigenvalues ω^- and ω^+ of the matrix

$$H = \overline{A} + \overline{B}\left(\mu_T^2 \boldsymbol{D}_0 - \overline{D}\right)^{-1} \overline{C} \qquad (32)$$

where

$$\overline{A} = \begin{bmatrix} A & 0 \\ C^T \boldsymbol{D}_0 C & -A^T \end{bmatrix}; \overline{B} = \begin{bmatrix} B \\ C^T \boldsymbol{D}_0 D - jC^T \boldsymbol{G}_0 \end{bmatrix}$$

$$\overline{C} = [\, D^T \boldsymbol{D}_0 C + j\boldsymbol{G}_0 C \quad -B^T \,]$$

$$\overline{D} = j\left(\boldsymbol{G}_0 D - D^T \boldsymbol{G}_0\right) + D^T \boldsymbol{D}_0 D$$

depending on the state space realization (A, B, C, D) of $M(s)$ and two scalings $\boldsymbol{G}_0$ and $\boldsymbol{D}_0$ satisfying (20) for $s = j\omega_0$.

4.4. Skewed and one-sided skewed μ methods

We do not detail these methods, which compute a skewed or one-sided skewed μ bound at a given frequency ω, and refer the interested reader to the following references:

- A skewed μ lower bound is presented in [10], whereas two different skewed μ upper bounds are presented in [10, 11, 13]. All three associated algorithms are polynomial-time, and the general case of a mixed model perturbation is considered.
- See [16] for a one-sided skewed μ upper bound. The method, which is polynomial-time, is applicable to a generic mixed model perturbation.
- See also [7] for exponential-time methods, which compute a lower and an upper bound of the real one-sided skewed s.s.v..

5. Example

To give an idea of how to use the above-mentioned tools and of how could look like the results of μ–analysis, we will apply *algorithms 1-4* to the example of the robustness analysis of the flexible space structures of [17].

It is a system of 70th order with parameter uncertainties on the 10 flexible modes. The real parameter uncertainties are normalized to the interval $\delta_i \in [-1;\ 1]$ by a value $\delta_{i,\max}$. They appear twice repeated, so that the perturbation matrix Δ is of size 20×20.

5.1. Lower bounds

The results of the μ lower bound computation are given in *figure 11*. The $*$ represent its two peaks calculated by *algorithm 1* and the o those by *algorithm 2*. Both algorithms deliver almost identical results. The higher peak of the lower bound appears with $\mu = 0.47$ at a frequency of $8.2\,\mathrm{rad}/s$, its robustness margin is $k_{\max} = 1/\mu = 2.13$. Hence, the δ_i can vary between $[-2.13;\ 2.13]$ before the system becomes unstable, i.e. the system remains stable within the expected range of the parameters $\delta_{i,\max}$, it is robust. On the other hand, if $k_{\max}$ becomes smaller than 1 ($\mu > 1$), the system becomes unstable within the parameter range for a certain combination of the δ_i. This critical perturbation Δ is directly delivered by both algorithms. The feedback of Δ with $M(s)$ gives the so-called worst-case, the system's configuration which is first destabilized and for which an improved control design should be elaborated.

We initialize *algorithm 1* with just the system and the uncertainty structure. For *algorithm 2* a vector of frequencies has additionally to be defined.

The *SPA* of [30] implemented in the `mu` command of MATLAB does not converge on the tested frequency band when launched with standard options and 100 frequency points to check. With more frequency points and more accurate options, it should converge as well, but the computation time increases immediately to unacceptable values. Furthermore, the initial problem remains that because of the gridding, a narrow, high peak can still be missed. It is initialized with the system, the uncertainty structure and a vector of frequencies.

5.2. Upper bounds

`mu` does not only compute a lower, but also an upper bound (using [27]) on the tested frequency band. As

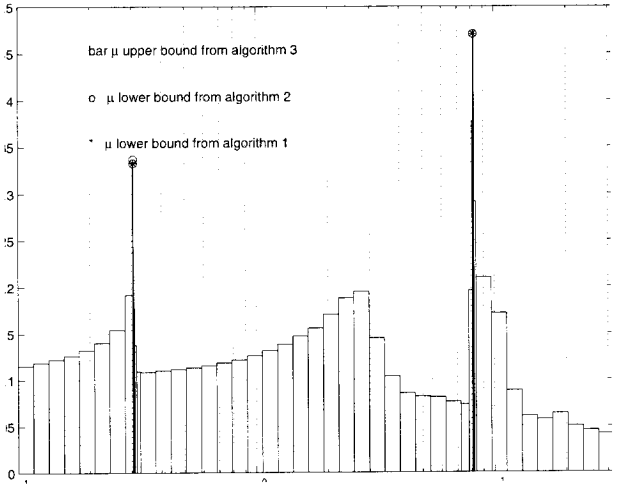

Figure 11. μ–plot for flexible space structures.

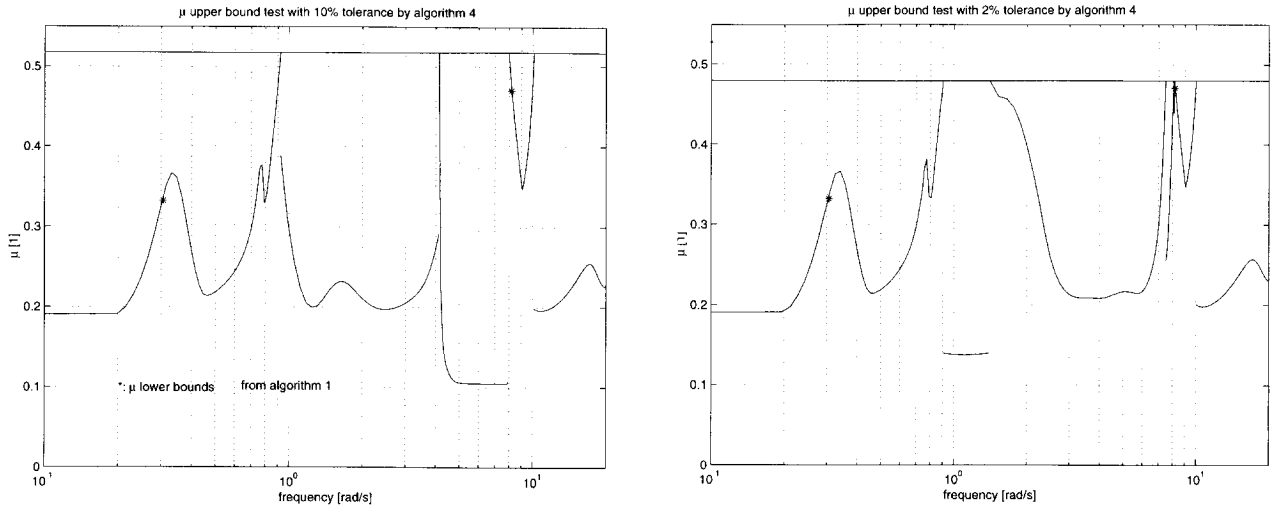

Figure 12. μ upper bound test (a) with 10 % tolerance (b) with 2 % tolerance.

before, launched with standard options and 100 frequency points, this upper bound is known to be too conservative for real uncertainties. With more points and more accurate, but too time-consuming options, it should deliver similar results for the upper bound, as in *figure 11* when it does not miss the peak because of gridding.

The bars in *figure 11* represent the frequency intervals where μ is inferior to the value given by the bar height. That is the result of *algorithm 3*. At both peaks the upper bound is very close to the lower bound, the difference is about 0.5 %, hence no conservatism. Hence, the exact value of μ is tightly determined. Not only is a worst-case identified, but robustness is ensured as well.

Similar conclusions can be drawn from the results of *algorithm 4* in *figure 12a* and *figure 12b*. The $*$ represent again the peaks of the lower bound given by *algorithm 1*. Starting from these peaks, the intervals are eliminated where μ is inferior to the test value (horizontal line) $\mu_T = 1.1 \max(\mu)$ ($\mu_T = 1.02 \max(\mu)$ respectively) with constant scalings $\boldsymbol{D}_0$ and $\boldsymbol{G}_0$. One curve starting at low μ values and reaching μ_T corresponds to one set of $\boldsymbol{D}_0$ and $\boldsymbol{G}_0$.

In both cases all intervals can be eliminated, so that on the tested frequency band, $\mu_T = 0.52$ (or $\mu_T = 0.48$ respectively) is an upper bound of the exact value of μ. In the case of 10 % tolerance 5 scalings have to be determined, in the case of 2 % tolerance 10 scalings. The additional scalings are located around the peak value of the lower bound. Hence, the more exact the upper bound is, the more time-consuming is the computation. This explains the higher computation times of the algorithm given in [27] as it determines scalings for each treated frequency point. For flexible structures a lot of points are necessary to track narrow, high peaks, so typical ratios of scalings (and hence in computation time) will be about 1/500 in favor of *algorithm 4*.

The initialization of algorithm 4 is done by the system, the uncertainty structure, the frequencies corresponding to the peak values of the lower bound and finally by limit frequencies defining a range where to check μ_T.

Algorithm 3 is initialized by the system, the uncertainty structure, the N frequency points treated simultaneously (here $N = 2$), a vector of initial frequencies and the desired tolerance. Remark: 40 initial points are largely sufficient as the algorithm itself refines the intervals where necessary (see the different bar widths in *figure 11*). Finally, about 50 scalings have to be computed.

6. Conclusions

This article gives an idea of what are the μ-measure and its derivatives and how they could be used for aeronautical applications: e.g. the determination of control law robustness of flexible structures, the determination of phase and delay margins and linear and non-linear analysis of PIO effects. The example shows how to use the algorithms and how to interpret their results. Hence, this article should rather be understood as an invitation to use these new methods in flight control analysis and design. For a deeper insight we refer to the detailed reference section.

References

[1] Bennani S., Looye G., Scherer C., Tutorial Part: μ-Synthesis, in: Magni J.-F., Bennani S., Terlouw J. (Eds.), Robust flight control – A design challenge, Springer Verlag, Berlin, Heidelberg, New York, London, Paris, Tokyo, 224, 1997, pp. 81–101.

[2] Boyd S., El Ghaoui L., Feron E., Balakrishnan V., Linear Matrix Inequalities in system and control theory, 1st ed., SIAM, Philadelphia, Pennsylvania, USA, Studies in Applied Mathematics, 15, 1994.

[3] Dailey R.L., A new algorithm for the real structured singular value, in: Proceedings of the ACC, 1990, pp. 3036–3040.

[4] Döll C., Magni J.-F., Looye G., Bennani S., Robustness analysis applied to autopilot design. Part 2: Evaluation of a new tool for μ-analysis, in: ICAS Congress, Melbourne, Australia, 1998.

[5] Duda H., Prediction of pilot-in-the-loop oscillations due to rate saturation, J. Guid. Control Dynam. 20 (3) (1997) 581–587.

[6] Duda H., Duus G., New handling qualities database on PIO due to rate saturation, Forschungsbericht 97–53, Institut für Flugmechanik, DLR Braunschweig, Porz-Wahnheide, Linder Höhe, Koln,1997.

[7] Ferreres G., A practical approach to robustness analysis with aeronautical applications, Book submitted, 1998.

[8] Ferreres G., Biannic J.M., A μ analysis technique without frequency gridding, Proceedings of the ACC, 1998.

[9] Ferreres G., Biannic J.M., Reliable computation of the robustness margin for a flexible transport aircraft, submitted, 1998.

[10] Ferreres G., Fromion V., Robustness analysis using the ν tool, Proceedings of the IEEE CDC, 4, 1996, pp. 4566–4570.

[11] Ferreres G., Fromion V., Computation of the robustness margin with the skewed μ tool, Syst. Control Lett. 32 (1997) 193–202.

[12] Ferreres G., Fromion V., Nonlinear analysis in the presence of parametric uncertainties, Int. J. Control 69 (5) (1998) 695–716.

[13] Ferreres G., FromionV., A new upper bound for the skewed structured singular value, to be published in: Int. J. Robust Nonlin. 1998.

[14] Ferreres G., Scorletti G., Robustness analysis in the presence of time delays, in: Proceedings of the IFAC workshop on linear time delay systems, 1998.

[15] Ferreres G., Fromion V., Duc G., M'Saad M., Application of real/mixed μ computational techniques to a H_∞ missile autopilot, Int. J. Robust Nonlin. 6 (8)(1996) 743–769.

[16] Ferreres G., Scorletti G., Fromion V., Advanced computation of the robustness margin, Proceedings of the IEEE CDC, 4, 1996, pp. 4580–4584.

[17] Frapard B., Girouart B., Döll C., Magni J.-F., Chiappa C., Mixed μ-analysis for flexible systems, Part II: Application to the SPOT family of earth observation satellites, IFAC World Congress, 1999.

[18] Helmersson A., Methods for robust gain scheduling, Ph.D. Thesis, Linkoping University, 58183 LINKÖPING, Sweden, 1995.

[19] Jones R.D., Structured singular value analysis for real parameter variations, in: Proceedings of the AIAA GNC Conference, USA, 1987, pp. 1424–1432.

[20] Magni J.-F., Multimodel eigenstructure assignment in flight-control design, Aerospace Sciences and Technology 3 (3) (1999).

[21] Magni J.-F., Döll C., A new simple lower bound of the mixed structured singular value, in: Asian Control Conference, Seoul, Korea, I, 1997, pp. 847–850.

[22] Magni J.-F., Döll C., Robustness analysis for flexible structures, Note to presentation at Journée du Groupe Commande robuste at LAAS, Toulouse, France, 1998.

[23] Magni J.-F., Manouan A., Robust flight control design by eigenstructure assignment, in: Proceedings of the IFAC Symposium on Robust Control, Rio de Janeiro, Brasil, I, 1994, pp. 388–393.

[24] Magni J.F., Le Gorrec Y., Chiappa C., A multimodel-based approach to robust and self-scheduled control design, P. IEEE CDC, 1998.

[25] Magni J.-F., Döll C., Chiappa C., Frapard B., Girouart B., Mixed μ-analysis for flexible structures. Part 1: Theory, in: IFAC World Congress, 1999.

[26] Newlin M.P., Young P.M., Mixed μ problems and branch and bound techniques, in: Proceedings of 31st IEEE Conference on Decision and Control,Tucson, Arizona, USA, 1992, pp. 3175–3180.

[27] Packard A., Doyle J., The complex structured singular value, Automatica 29 (1) (1993) 71–109.

[28] Tierno J.E., Young P.M., An improved μ lower bound via adaptive power iteration, in: Proceedings of 31st IEEE Conference on Decision and Control, Tucson, Arizona, USA, 1992, pp. 3181–3186.

[29] Varga A., Looye G., Moormann D., Grübel G., Automated generation of LFT-based parametric uncertainty descriptions from generic aircraft models, Mathematical Modelling of Systems 4 (4) (1999) 249–274.

[30] Young P.M., Doyle J.C., Computation of μ with real and complex uncertainties, P. IEEE CDC (1990) 1230–1235.

[31] Young P.M., Newlin M.P., Doyle J.C., Computing bounds for the mixed μ problem, Int. J. Robust Nonlin. 6 (5) (1995) 573–590.